

Glyoxylic-Acetal-Based Electrolytes for Sodium-Ion Batteries and Sodium-Ion Capacitors

Christian Leibing,^[a, b] Desirée Leistenschneider,^[a, b] Christof Neumann,^[b, c] Martin Oschatz,^[a, b] Andrey Turchanin,^[b, c] and Andrea Balducci^{*,[a, b]}

A comprehensive study on the properties and implementation of glyoxylic-acetals in sodium-ion energy storage systems is presented. Electrolytes containing 1,1,2,2-tetramethoxyethane (tetramethoxyglyoxal, TMG), 1,1,2,2-tetraethoxyethane (tetraethoxyglyoxal, TEG) and a mixture of the latter with propylene carbonate (PC) exhibit increased thermal stabilities and higher flash points compared to classical electrolytes based on carbonates as solvents. Due to its favorable properties, 1 M NaTFSI in TEG/PC (3:7), has been selected and used for sodium-ion energy storage systems based on a Prussian Blue (PB) positive electrode and a hard carbon (HC) negative electrode.

Compared to conventional electrolyte (based on a 1:1 mixture of ethylene carbonate, EC, and dimethyl carbonate, DMC), this glyoxylic-acetal electrolyte provides competitive capacity and prolonged cycle life. Postmortem XPS analysis indicates that the electrode-electrolyte interphases formed in presence of TEG are thicker and presumably more protective, inhibiting typical degradation processes of the electrodes. Furthermore, it is demonstrated that the suitable properties of TEG on the cycling stability can also be exploited for the construction of highly stable sodium-ion capacitors.

Introduction

Nowadays mobile energy storage devices largely rely on lithium-ion technology, but resource demands and raise of the predicted cost intensified the research effort on other alkali metal ion batteries. Sodium-ion batteries (NIBs) are being investigated alongside their Li competitors since the 1980's.^[1] Although their theoretical energy density is naturally lower, NIBs offer advantages in terms of availability of mineral resources and cost.^[2] The larger number of employable transition metals and wider variety of possible compounds and structures for their insertion electrodes offers the chance to solve the problems associated with the supply, cost, and toxicity of transition metals used in LIBs.^[3] Throughout the last


decade, great advances have been made in the field of electrode materials, which ultimately started the commercialization process.^[2,4] However, a seemingly often underestimated key role for their (further) development comes to the electrolyte, since its properties largely determine the performance of the whole battery. The electrolyte is not only responsible for facilitating the ion transport between the electrodes, while simultaneously electronically insulating them. In addition, the electrolyte will dictate the chemistry of the interphases formed on the electrodes, which (co-) determine the practical capacity, rate capability, and lifetime of the overall battery system.^[5] Moreover, it directly (by its flammability and volatility) and indirectly (by the stability of the interphases) sets the tolerance limit to chemical and thermal stress, i.e., it impacts the safety of the alkali-metal-ion battery.


Addressing the latter point, we proposed the use of glyoxylic-acetals as alternative electrolyte solvents for lithium and potassium ion batteries. Tetraethoxyglyoxal (TEG, IUPAC: 1,1,2,2-tetraethoxyethane) and tetramethoxyglyoxal (TMG, IUPAC: 1,1,2,2-tetramethoxyethane) are the full acetals of glyoxal (IUPAC: ethanedial) and can be obtained from the latter via a condensation reaction with methanol or ethanol.^[6] TEG and TMG are commercially available and their price is comparable to other solvents currently used in energy storage devices.^[7] In addition, both have a very low toxicity (LD₅₀ rat > 2000 mg kg⁻¹) and are classified as harmless in terms of environmental hazards. Previous areas of application for these compounds are mainly solution-based chemical processes, for example the production of varnishes and paints.^[8] Although acetals such as TEG and TMG do not have very high dielectric constants, they exhibit low viscosities, very low melting points and good solubility for a wide range of salts. However, a key characteristic is that the thermal stabilities, boiling points, and flash points of TEG and TMG are much higher than those of linear carbonate


[a] C. Leibing, Dr. D. Leistenschneider, Prof. Dr. M. Oschatz, Prof. Dr. A. Balducci
Institute for Technical Chemistry and Environmental Chemistry
Friedrich Schiller University Jena
Philosophenweg 7a, 07743 Jena (Germany)
E-mail: andrea.balducci@uni-jena.de

[b] C. Leibing, Dr. D. Leistenschneider, Dr. C. Neumann, Prof. Dr. M. Oschatz,
Prof. Dr. A. Turchanin, Prof. Dr. A. Balducci
Center for Energy and Environmental Chemistry Jena (CEEC Jena)
Philosophenweg 7a, 07743 Jena (Germany)

[c] Dr. C. Neumann, Prof. Dr. A. Turchanin
Institute of Physical Chemistry
Friedrich Schiller University Jena
Lessingstraße 10, 07743 Jena (Germany)

 Supporting information for this article is available on the WWW under <https://doi.org/10.1002/cssc.202300161>

 This publication is part of a joint Special Collection of ChemSusChem, Batteries & Supercaps, and Energy Technology including invited contributions focusing on the "International Conference on Sodium Batteries (ICNaB)". Please visit chemsuschem.org/collections to view all contributions.

 © 2023 The Authors. ChemSusChem published by Wiley-VCH GmbH. This is an open access article under the terms of the Creative Commons Attribution Non-Commercial License, which permits use, distribution and reproduction in any medium, provided the original work is properly cited and is not used for commercial purposes.

solvents, which are widely used in conventional electrolyte formulations.^[7] Due to all these properties, their use in energy storage systems appears promising. We demonstrated that TMG and TEG provide intrinsic film-forming ability and form a suitable solid electrolyte interphase (SEI) layer on graphite, soft carbon and hard carbon (HC) electrodes.^[9] Furthermore, the properties of the interphase formed by TEG on Si/graphite electrodes lead to a higher retention of silicon and graphite activity and thus prolong the cycle life.^[10] Beneficial effects compared to conventional electrolytes have also been found for Fe₂O₃-carbon composite electrodes when increasing the cycling temperature to 60 °C.^[11] Based on these findings, glyoxylic-acetals, in pure form and in mixtures with carbonate solvents, have been successfully utilized in lithium and potassium ion full cells using lithium iron phosphate (LFP) and lithium nickel manganese cobalt oxide (NMC) or respectively Prussian white as cathode materials.^[12]

We recently demonstrated that a mixture of TEG and PC can also be used in sodium-ion half-cells with HC anodes.^[13] However, a comprehensive study on the properties and implementation of glyoxylic-acetals in sodium-ion energy storage systems is still lacking. In this work, we therefore focus on three electrolytes containing TMG, TEG as well as TEG/PC (3:7) as solvents and sodium bis(trifluoromethanesulfonyl)imide, NaTFSI, with a concentration 1 mol L⁻¹ (1 M) as conductive salt, which are analogue to the formulations that have been previously investigated in lithium-ion systems.^[7,9a,b,12b] On basis of their properties regarding thermal and electrochemical stability, conductivity, and viscosity, one of the three electrolytes is selected for a comparative study towards application in sodium-ion batteries, using 1 M NaTFSI in EC/DMC (1:1) as reference electrolyte. By this, we show that glyoxylic-acetal-containing electrolytes have a positive impact on the cycling stability of Na-ion batteries with Prussian Blue positive electrodes and HC negative electrodes. As the performance of the battery is largely influenced by the chemistry of the interphases, its relation to electrochemical key parameters is assessed for the electrolytes under investigation.

Experimental Section

Electrolyte characterization

1,1,2,2-Tetramethoxyethane (TMG) and 1,1,2,2-tetraethoxyethane (TEG) were supplied by WeylChem. For purification, the solvents were filtered over dried aluminum oxide (90 active basic, Merck) under argon atmosphere. By this, their water content was reduced to ≤20 ppm (determined by Karl-Fischer titration at an C20 Coulometric KF Titrator, METTLER TOLEDO) and the butylated hydroxytoluene stabilizer was removed. Propylene carbonate (PC, anhydrous 99.7%, Sigma Aldrich), ethylene carbonate (EC, battery grade, Fujifilm) and dimethyl carbonate (DMC, ≥99%, Sigma Aldrich) have been used without further purification. The electrolytes were prepared in an argon filled glovebox (MBraun O₂ and H₂O < 1 ppm) using 1 M sodium bis(trifluoromethanesulfonyl)imide (NaTFSI, purchased from Solvionic) as conductive salt. The binary solvent mixtures were prepared referring to their mass ratio. The viscosity was measured in the temperature range between -30-

80 °C at an Anton-Paar MCR 102 rotational viscometer, applying a shear rate of 1000 s⁻¹. For conductivity measurements, 500 μL of the electrolyte were added into a sealed glass cell with two perfectly parallel platinized platinum electrodes with a known cell constant (around 1 cm⁻¹, examined with KCl solution). The cell was placed into a climate chamber (BINDER) for electrochemical impedance measurement (amplitude: 5 mV, frequencies range: 100 mHz to 100 MHz) using a ModulabXM ECS potentiostat (Solartron) to obtain the alternating current resistance and calculate the electrolyte conductivity. Thermogravimetric analyses were performed on a Perkin Elmer STA 6000 with nitrogen as carrier gas and a flow rate of 20 mL min⁻¹. A heating rate of 10 °C min⁻¹ was applied in dynamic measurements; isothermal measurements were conducted at 60 °C. The flashpoints of the electrolytes were measured at a NORMALAB NPV 310 with gas ignition using 2 mL of solvent in the rapid equilibrium closed cup method according to ISO 3679.

The electrochemical stability window (ESW) of the electrolytes was measured in three electrode Swagelok cells using a circular Pt-disc as working electrode (WE), a freestanding oversized activated carbon electrode as counter electrode (CE) and a silver wire as reference electrode (RE). The glass-fiber separator of the cells (Whatman GF/D) was soaked with 150 μL of electrolyte and the cells were applied to linear sweep voltammetry measurements with a scan rate of 1 mV s⁻¹ at an VMP-3 or MPG-2 (BioLogic). The threshold for the electrochemical stability was defined as 100 μA for the resulting current.

Electrochemical testing

The hard carbon (HC) material was synthesized from sucrose by a previously described method.^[9b] Its characterization is provided in Figure S1 of the Supporting Information (SI). To prepare electrodes for half cell measurements, 90% of HC, 5% carbon black (C-ENERGY™ Super C65, Imerys) and 5% carboxymethyl cellulose (CMC, CRT2000GA, Walocel) were mixed with water in a solid to liquid mass ratio of 3:8. For the full cell measurements, the material ratio within the HC composite electrode was changed to 85% of HC, 5% carbon black and 10% CMC binder, to increase the mechanic stability of the electrode for the pre-cycling/pre-sodiation process and subsequent reassembly into the full cell. The resulting slurries were casted onto dendritic copper foil applying a film thickness of 120 μm for half cells or 150 μm for full cells. Activated carbon (Kuraray YP80-F) electrodes were prepared using the 85:5:10 protocol for slurry preparation. Instead of copper, KOH-etched aluminum foil was used as a current collector. A film thickness of 600 μm was applied for electrode casting. Etching of the Al-current collector was performed by immersing the foil in a 5 M aqueous KOH solution at 60 °C for 1 min. By this, an artificial passivation layer was formed, and the surface roughness was increased to improve the adhesion of the electrode material. The Prussian Blue (PB) electrodes contained 80% of active material, 10% of CMC binder and 10% of carbon black and were coated onto aluminum foil, with a wet film thickness of 100 μm for half cells and 400 μm for full cells. After drying under air atmosphere, electrodes with a diameter of 12 mm were cut from the films and vacuum-dried at 80 °C in a micro glass oven (Büchi) for 6 h. Subsequently, the electrodes were weighted, dried again, and transferred into an argon filled glovebox (MBraun O₂ and H₂O < 1 ppm).

For electrochemical characterizations, three-electrode Swagelok cells were assembled inside the glovebox using 150 μL of electrolyte and a glass-fiber separator (Whatman GF/D). In case of the half cells, Na-metal was used as counter and reference electrode. The active material mass loading in the half cells was around 2.5 to 2.8 mg cm⁻² for the HC electrodes and 0.7–0.8 mg cm⁻² in case of the PB electrodes. At the beginning of the cycling protocol, PB half

cells were discharged with a current density of 9.3 mA g^{-1} for sodiating the material. The HC half cells were applied to an SEI formation protocol to eliminate the irreversible capacity in the first cycles. In this protocol, the cells are discharged with 0.05 C for 3 h, followed by discharging to 0.005 V vs. Na/Na⁺ with 0.1 C. Subsequently, the cells are charged with 0.1 C to 2.5 V vs Na/Na⁺, discharged with 0.025 C to 0.005 V vs. Na/Na⁺ and finally recharged with 0.1 C to 2 V vs. Na/Na⁺. A comparison to half-cells that have been tested without this protocol is provided in Figure S2 of the SI. Galvanostatic intermittent titration technique (GITT) measurements of the HC electrodes were carried out following a previously described method.^[9b]

To assemble sodium-ion battery full cells, PB electrodes with a mass loading of 2.7 mg cm^{-2} have been pre-sodiated in half cells by galvanostatic cycling with potential limitation (GCPL) for 5 cycles at an Arbin Instruments LBT21084 in a voltage range from 2.0–3.8 V vs Na/Na⁺ applying a current rate of 37 mA g^{-1} . Also, the HC electrodes have been pre-formed in half cells, applying the afore mentioned SEI formation protocol. The pre-cycled electrodes were assembled into three electrode Swagelok cells with Na-metal as reference electrode. The cells were connected to a BioLogic VMP-3 or BioLogic MPG-2 Potentiostat and tested on GCPL applying currents of 37, 182 and 372 mA g^{-1} according to the mass of the negative electrode. The potentials of both electrodes were controlled. In case of the positive electrode, the limits were set to 2.0–3.8 V vs Na/Na⁺ and in case of the anode to 0.05–2.0 V vs Na/Na⁺.

Sodium-ion capacitors (NICs) were assembled following a comparable procedure: Activated carbon electrodes were pre-cycled (GCPL) in half-cells at an Arbin Instruments LBT21084 in a potential range from 2–3.8 V vs Na/Na⁺, applying a current rate of 1 A g^{-1} . The cycling was stopped at the maximum potential. HC electrodes were pre-sodiated by applying the SEI formation protocol^[9b] and discharging the half-cell to 0.005 V. After assembly in the glovebox, the full cell containing a Na-metal reference electrode was connected to a BioLogic VMP-3 or BioLogic MPG-2 Potentiostat for GCPL measurements. The potentials of both electrodes were controlled analog to the sodium-ion battery full cell. The potential limitations and currents were selected analog to the sodium-ion battery full cell.

Post-mortem analysis

For post-mortem analysis, the respective cells were disassembled in the glovebox and the electrodes were washed by 1 min submersion in the respective electrolyte solvents TEG/PC and DMC for the EC/DMC cells, to remove salt residues from the surface. The washed electrodes were dried in a vacuum glass oven at 1×10^{-2} mbar for at least 24 h. X-ray photoelectron spectroscopy (XPS) analysis was conducted for samples of the pristine electrodes using a Thermo Scientific KAlpha spectrometer. The spectrometer was equipped with an Al K α anode ($h\nu = 1486.6 \text{ eV}$) as the X-ray source. The chamber pressure during each measurement did not exceed 5×10^{-8} mbar. To compensate potential surface charge, which occurs due to electrically insulating species, a flood gun was used. Survey scans were recorded with a step size of 1 eV and a pass energy of 100 eV and used to determine the surface's elemental composition. High resolution spectra were recorded with a step size of 0.05 eV with a pass energy of 30 eV. The samples of the cycled electrodes were measured using a UHV Multiprobe system (Scienta Omicron) equipped with a monochromatic X-ray source (Al K α) and an electron analyzer (Argus CU) with a spectral resolution of 0.6 eV. The XPS measurements were carried out at a pressure of $< 2 \times 10^{-10}$ mbar. An electron flood gun (NEK150SC, Staib, Germany) at 6 eV and $50 \mu\text{A}$ was used for charge compensation during data

acquisition. Survey scans were recorded with a step size of 0.5 eV and a pass energy of 50 eV, the high-resolution spectra were recorded with a step size of 0.05 eV and a pass energy of 30 eV. Binding energies were referenced to the C 1s at 284.6 eV as all samples contain graphitic carbon as a conductive additive. The resulting peak shifting values are given in the SI. All spectra were fitted using Voigt functions. For quantification, the relative sensitivity factors (RSF) of C 1s (1.00), O 1s (2.93), N 1s (1.80), Fe 2p_{3/2} (10.80), Na 1s (8.52), F 1s (4.43) and S 2p_{3/2} (1.11) were used.

Results and Discussion

Physicochemical characterization

As described before, glyoxylic-acetals offer advantages with respect to their thermal properties, especially when compared to linear carbonates that are widely used as co-solvents in conventional electrolytes for Li-, Na- and K-ion batteries.^[7,12a] To answer the question of how these properties are reflected in the thermal behavior of the resulting electrolytes, the thermogravimetric analysis of the 3 glyoxylic-acetal electrolytes and the EC/DMC reference electrolyte are displayed in Figure 1. Here, the glyoxylic-acetal-based sodium ion electrolytes behave comparable to their lithium counterparts.^[9b] They maintain 95% of their initial mass up to temperatures of 58 °C (1 M NaTFSI in TMG) to 97 °C (1 M NaTFSI in TEG/PC) in the dynamic measurement (Figure 1a). After complete evaporation of the solvents, the decomposition of the NaTFSI salt is initiated at around 400 °C, which is in good accordance^[14] with literature. When exposed to 60 °C (isothermal investigation, Figure 1b), a complete solvent evaporation is reached after 12 h in case of the TEG/PC electrolyte. Although the pure 1,1,2,2-tetramethoxyethane (TMG) and 1,1,2,2-tetraethoxyethane (TEG)-based electrolytes display a higher vapor pressure, they still offer a well visible improvement compared to electrolytes containing linear carbonates. 1 M NaTFSI in EC/DMC (1:1) shows the fast evaporation of highly volatile DMC. Already at 30 °C (starting point of the dynamic TGA measurement), the DMC evaporates from the solution, and only EC and the conductive salt are left. In addition to temperature induced solvent depletion, the flammability of the electrolyte is directly impacting the safety of the battery. While the flash point of 1 M NaTFSI in EC/DMC (1:1) is lower than the starting point of the measurement, the two TEG-containing electrolytes cannot be ignited at temperatures lower than 75 °C (see Figure 1c). Consequently, electrolyte leakage in a battery could not lead to fire by inflammation of the electrolyte under ambient conditions.

Figure 2 displays the viscosity and conductivity of the respective electrolytes in a temperature range from –30 °C to 80 °C. As already discussed in earlier articles, the viscosity and conductivity of the glyoxylic-acetal-based electrolytes at room temperature is clearly not superior compared to conventional formulations.^[7] At 20 °C, the conductivity is only 0.44 mS cm^{-1} for the TEG electrolyte and 1.73 mS cm^{-1} for the TMG electrolyte (Figure 2a). All conductivity and viscosity values are summarized in Table S1 of the Supporting Information (SI). Due to the high dielectric constant of propylene carbonate the mixture of TEG

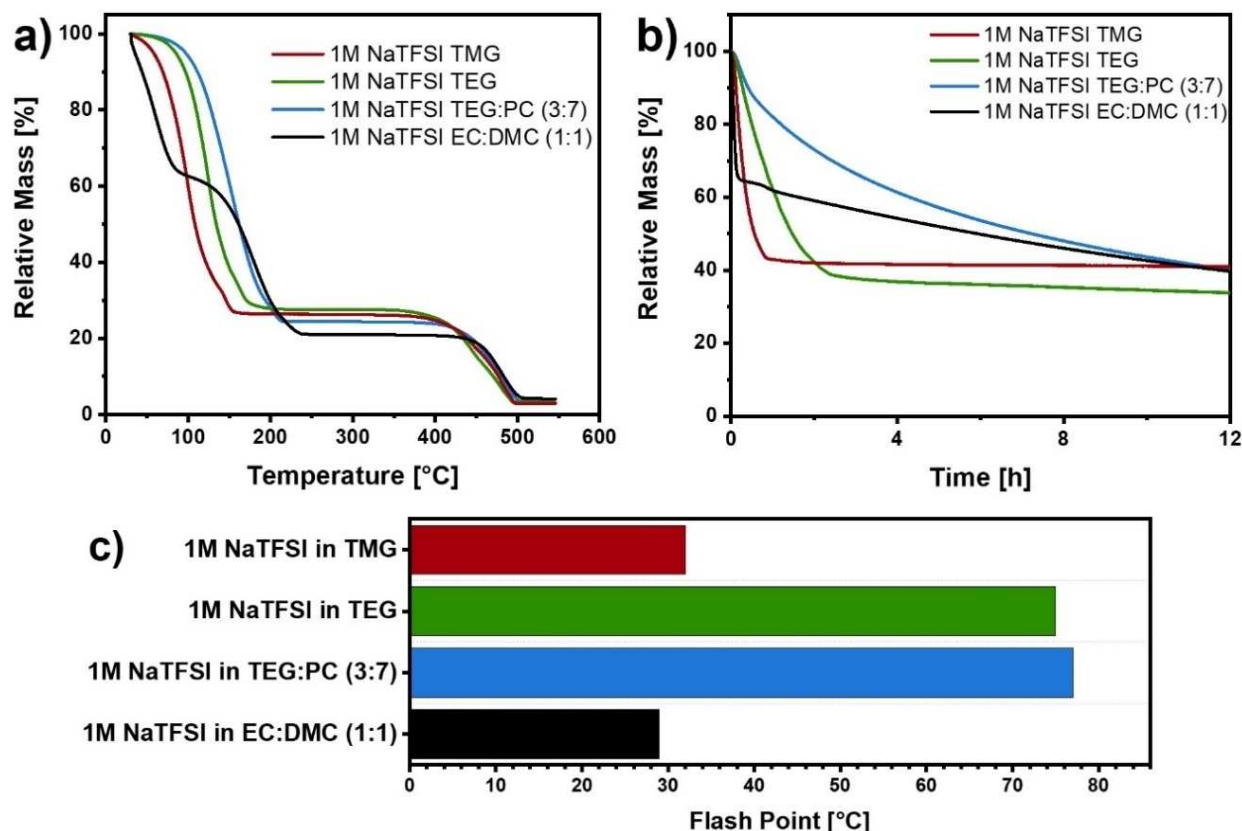


Figure 1. Thermogravimetric analysis: a) dynamic measurement (temperature increase of $10^{\circ}\text{Cmin}^{-1}$); b) isothermal measurement at 60°C , and c) flash points of glyoxylic-acetal-based electrolytes and 1 M NaTFSI in EC/DMC (1:1).

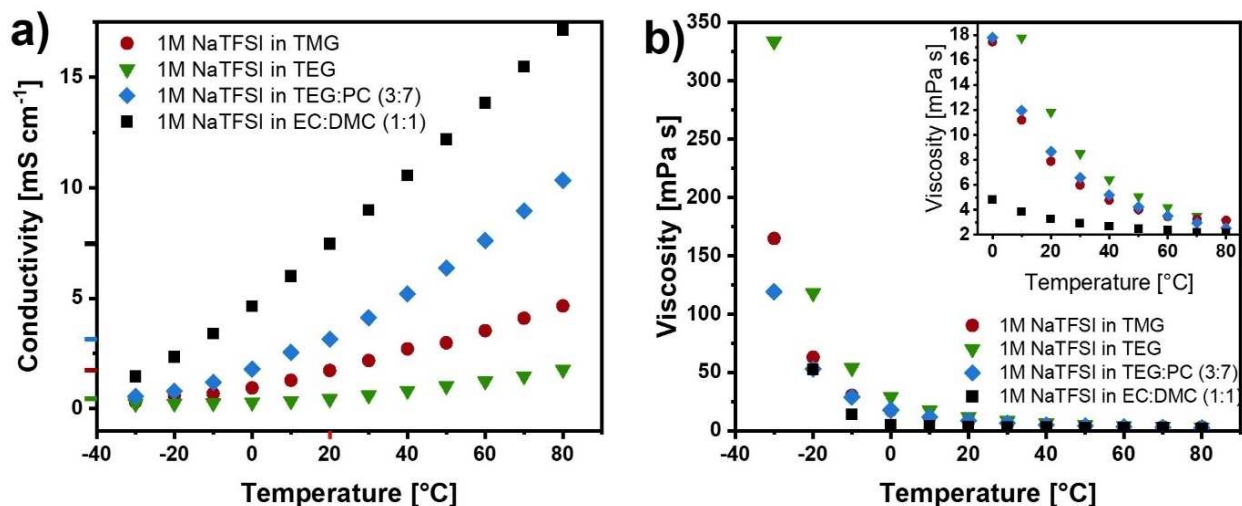


Figure 2. a) Conductivity and b) viscosity of NaTFSI-glyoxylic-acetal and EC/DMC electrolytes in a temperature range from -30 to 80°C .

and PC provides an increased ionic conductivity for the respective electrolyte (3.15 mS cm^{-1}) compared to the purely glyoxylic-based formulations. Interestingly, the viscosity of the electrolytes (Figure 2b) does not follow the same trends observed in the conductivity measurements. In the temperature range between 0°C and 60°C , 1 M NaTFSI in TMG displays the

lowest viscosity among the glyoxylic-containing electrolytes. Outside of this range, 1 M NaTFSI in TEG/PC (3:7) is least viscous. Although the neat PC solvent exhibits a higher viscosity than the neat TEG solvent (2.53 mPa s compared to 1.74 mPa s), the 1 M NaTFSI in TEG electrolyte is generally more viscous than the one based on the TEG/PC mixture. This has already been

observed for lithium electrolyte analogues and may be attributed to ion solvation effects.^[9b] Among the investigated electrolytes, 1 M NaTFSI in EC/DMC (1:1) displays the highest conductivity (8.67 mS cm^{-1} at 20°C) and the lowest viscosity (3.3 mPas). However, -30°C is close to crystallization temperature of this electrolyte.^[15] For this reason, the viscosity analysis was limited to -20°C for EC/DMC to not damage the measuring system with crystallized salt. Additionally, the difference between the TEG/PC and EC/DMC electrolytes in terms of conductivity is less than 0.5 mS cm^{-1} at -20°C , which underlines that glyoxylic-acetal-based electrolytes also offer good properties at low temperatures.

A drawback which is associated with many ether solvents is their limited electrochemical stability under high potentials.^[16] The electrolytes based on pure TMG and TEG are anodically stable up to 3.7–3.9 V vs. Na/Na^+ . Thus, they can be used in combination with low operative voltage positive electrode materials, such as PB analogues (PBAs) or sodium (Na) super ionic conductors (NASICONs).^[17] Though, many sodium transition metal oxides require electrolytes which are more stable against oxidation, since their upper cut-off potential is above 4 V vs. Na/Na^+ .^[18] As can be seen from Figure 3, this condition can be met by the addition of PC. In the TEG/PC electrolyte, the electrochemical stability is increased up to 4.3 V vs. Na/Na^+ . Considering this and afore discussed results regarding thermal stability, conductivity and viscosity, 1 M NaTFSI in TEG/PC (3:7) provides the most promising properties among the glyoxylic-acetal-containing electrolytes and was therefore selected for detailed electrochemical investigations.

Materials for the positive and negative electrode

As presented, positive electrode materials for sodium-ion batteries are more diverse compared to their Li-ion competitors. The range of useable transition metals comprises all elements

from Ti to Cu, leading to a high number of possible structures.^[3b] Main material classes that are considered for application include layered oxides, polyanionic compounds and PBAs.^[19] Being inspired by the pigment PB, $\text{Fe}_4[\text{Fe}(\text{CN})_6]_3$, the latter class of components comprises compounds with various crystal structures, depending on the type and ratio of the atomic species being incorporated. The composition of PBAs may be emphasized as $\text{A}_x\text{M}[\text{M}'(\text{CN})_6]_y \cdot z\text{H}_2\text{O}$ with A being one or more alkali metals or alkaline earth metals and M and M' representing transition metals, such as Mn, Fe, Co, Ni, Cu, Zn, etc.^[20] Depending on the type of transition metal(s), this class of sodium-ion batteries (NIBs) positive electrode materials can offer advantages in terms of cost and non-toxicity, while providing high cycling stability and rate capability. However, their performance is dependent on the crystal size and the amount of water incorporated in the crystal structure.^[21]

To compare the properties and performance of the glyoxylic-acetal-containing electrolyte to the one containing only organic carbonates, a rather simple, but robust and abundant material has been selected for the positive electrode, which is the original PB, $\text{Fe}_4[\text{Fe}(\text{CN})_6]_3$. As it can be seen from Figure 4a, PB exhibits a quasi-plateau for Na-intercalation between 3 and 2.5 V and provides only moderate capacity values, compared to other cathodic materials proposed for Na-ion. Though, it displays a good cycling stability and rate capability, owing to the excellent Na diffusion into the cubic face centered structure.^[22] Furthermore, this well-known pigment is readily available, inexpensive, and easy to process. Comparing the rate performance of the PB electrodes in combination with TEG/PC and EC/DMC electrolytes (Figure 4c, potential profiles: Figure S3 of the SI), only minor differences can be observed at current rates of 37, 186 and 372 mA g^{-1} . However, the Coulombic efficiencies reveal that the glyoxylic-acetal-containing electrolyte facilitates a much more reversible charge storage process, that will presumably lead to a higher cycling stability. This may be already indicated by considering the slope of the capacity over cycle number graphs in Figure 4e.

Different anodic material classes, including carbonaceous materials, alloys, Ti-based insertion electrodes, or conversion type materials, are subject to current research efforts.^[23] Among these, hard carbons (HC) remain the most relevant for practical application,^[2,4e,19a] due to their high energy density and simplicity in synthesis.^[23,24] In view of this, a sucrose-based HC material was chosen as negative electrode for the implementation of the TEG/PC electrolyte in Na-ion batteries. Respective half-cell measurements are displayed in Figure 4b, d and f. The capacity achieved in this measurement is comparable to the one of the PB electrodes discussed before and thus rather low for such a carbonaceous material. This is, among others, related to the lack of plateau capacity at currents of 186 mA g^{-1} and above (potential profiles at all current densities are displayed in Figure S4). As indicated by the GITT analysis in Figure S5 of the SI, the strongly decreasing diffusivity of Na-ions into the carbon material may be a reason for the potential-plateau occurring at $< 50 \text{ mV}$, which is below the cutoff-potential in this experiment. Nevertheless, this material can be utilized as a reference to

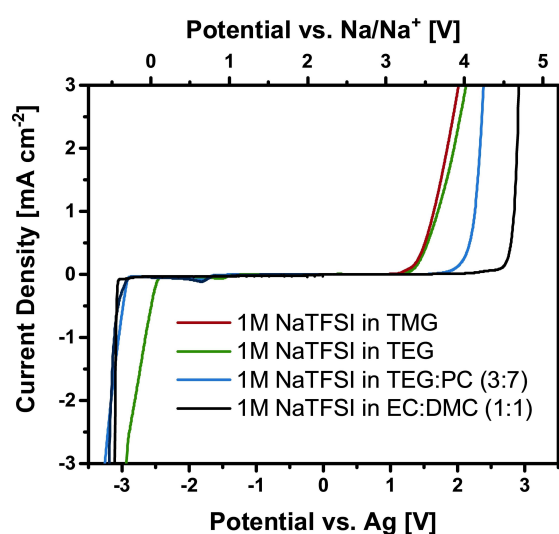


Figure 3. Electrochemical stability window of NaTFSI-glyoxylic-acetal and EC/DMC electrolytes.

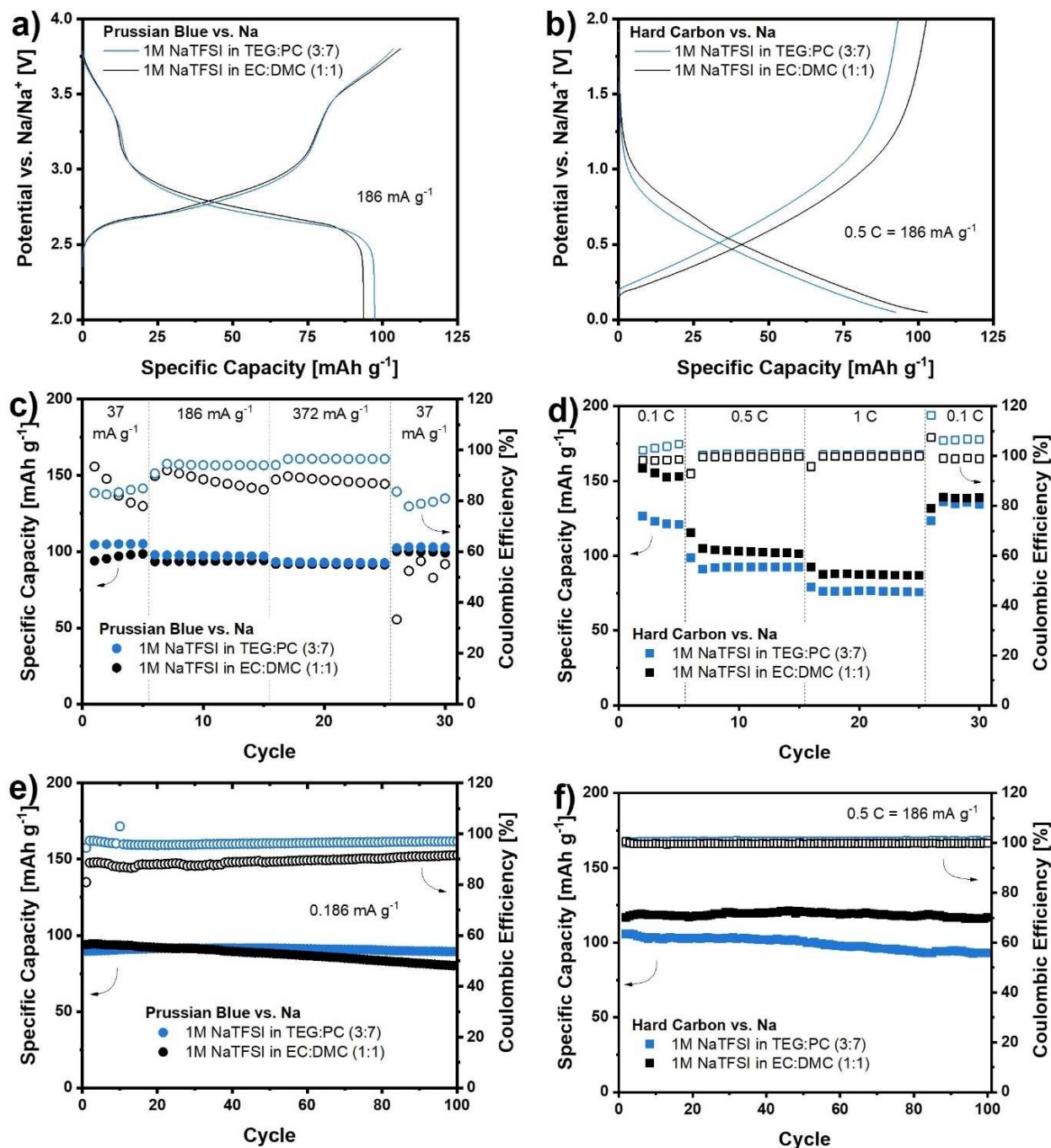


Figure 4. Voltage profiles, rate capability, and cycling stability and of PB vs. Na metal (a, c, e) and HC vs. Na metal half cells (b, d, f) with 1 M NaTFSI in TEG/PC (3:7) and 1 M NaTFSI in EC/DMC as electrolyte.

investigate and compare the interaction of glyoxylic-acetal and organic carbonate electrolytes with carbonaceous electrodes. In half-cells vs. Na metal as counter and reference electrode, the TEG/PC electrolyte enables a capacity retention of 89% from cycle 2 to cycle 100 at 186 mA g⁻¹ (Figure 4f). Also, the coulombic efficiency of 99–100% indicates a good reversibility of the process without major degradation of the electrode or electrolyte. The capacity and capacity retention in 1 M NaTFSI in EC/DMC (1:1) is slightly higher, especially in the early cycles at

a low current density of 37 mA h g⁻¹. As already pointed out, this is connected to the exploitation of plateau capacity, which is initially higher in the EC/DMC electrolyte.

Another important parameter for HC materials is the initial coulombic efficiency (ICE), especially when it comes to full cell application. The consumption of Na-ions by interphase formation on the negative electrode, as well as irreversible binding of Na-ions inside the carbon host, limits the practical capacity of the battery. Hence, besides the electrolyte, the carbon material

itself, its microstructure, surface area and surface functional groups have a major impact on the ICE. As can be seen from Figure S2 of the SI, both electrolytes, TEG/PC and EC/DMC, have an ICE of 53%. To reduce the contribution of irreversibly bound charge carriers in our measurements, especially in view of the full cell measurements presented in the next paragraph, an SEI formation procedure, described in our previous work has been applied to the HC electrodes in the full cell and to those in the half cell, presented in Figure 4b, d and f. By comparison to the HC half cells in Figure S2 of the SI that have not been applied to this pretreatment protocol, the irreversible capacity in the first cycles is effectively eliminated.

Sodium-Ion batteries and sodium-ion capacitor

The tests in half cells have proven that the selected glyoxylic-acetal electrolyte, 1 M NaTFSI in TEG/PC (3:7) can be successfully utilized in combination with PB and HC. In both cases this results in capacities, rate capabilities and cycling stabilities competitive to an electrolyte consisting of the same conductive salt in a binary organic carbonate solvent mixture. On this basis, lab-scale sodium-ion battery test cells (3-electrode Swagelok cells) have been constructed using both electrolytes. All the details about the electrode-pre-cycling processes that are necessary to introduce Na ions into the system, are reported in the experimental section. The results of the rate capability measurements and long-term cycling are shown in Figure 5. The cell with EC/DMC displays higher specific capacities (related to the mass of both electrodes) at all current densities applied (Figure 5a). At 0.037 A g^{-1} , the capacity with TEG/PC is around 80% of the capacity obtained with EC/DMC. On the one hand this originates from the fact that the PB electrode was over-capacitive in the full cell and the HC exhibits a higher capacity with EC/DMC. On the other hand, SEI resistivity effects may be less pronounced in the carbonate electrolyte, as will be discussed in context with the XPS measurements. Although the capacity of the TEG/PC cell is initially lower, the system stabilizes in the long-term charge-discharge experiment (Fig-

ure 5b) and can be cycled over 1000 cycles without major capacity fading. It shall be mentioned at this point, that this lab-scale cell is so far not optimized at all. Neither the electrode composition, i.e., the ratio and type of binder or conductive additive, nor the mass balancing of the electrodes in the full cell have been studied in all detail. In view of this, the positive impact of the glyoxylic-acetal-containing electrolyte on the cycling stability of the PB-HC full cell, seems promising. The slight capacity (re)-gain after the first 250 cycles in this cell may be attributed to a decrease in resistivity at the HC electrode, as can be concluded from the potential profiles of the cell in Figure S6 of the SI. In comparison to this, the EC/DMC-containing full cell falls behind in terms of capacity after around 100 cycles at 186 mA g^{-1} .

On the way towards understanding the different cycling stabilities of glyoxylic-acetal-containing and carbonate-based electrolytes, disassembly of the Swagelok cells after 1000 charge-discharge cycles (Figure 5b) revealed first differences that could already be observed by eye: The separators of the EC/DMC-containing cells show an orange to brown discoloration, whereas those of the TEG/PC cells are still white, as can be seen in Figure S8 of the SI. This indicates the presence of decomposition products within the bulk electrolyte, in case of EC/DMC, which could originate from the instability of metallic sodium in the electrolyte. Besides the properties of the bulk electrolyte that may be altered by aging effects, the chemistry of the interphases is of utmost importance for the performance and lifetime of the battery. Therefore, the electrodes were disassembled under inert atmosphere, and characterized by postmortem XPS. For a better comparison, non-cycled electrodes of PB and HC are taken as a reference. The elemental composition of the electrode surfaces is shown in Figure 6. In its pristine state, the surface of the HC electrode mainly consists of carbon and oxygen. Upon cycling, an SEI layer is established, resulting in a decrease of measurable carbon content and the occurrence of fluorine and sulfur, as well as an increase of Na on the electrode surface. Comparing the electrodes cycled in the two different electrolytes, it is apparent that this effect is more pronounced in TEG/PC. Thus, it can be concluded that the

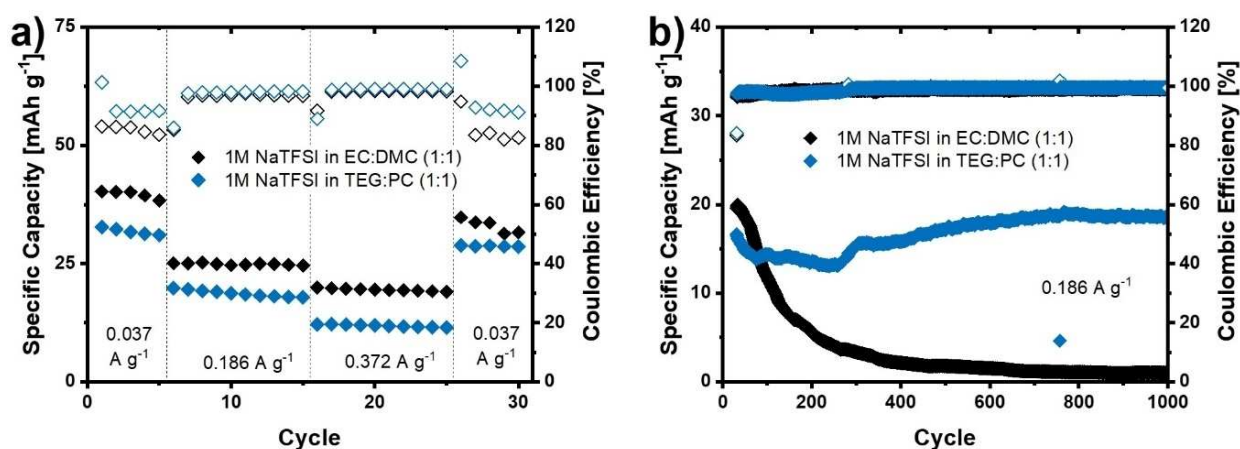


Figure 5. a) Rate capability and b) cycling stability of sodium-ion battery full cells with 1 M NaTFSI in TEG/PC (3:7) and 1 M NaTFSI in EC/DMC as electrolyte.

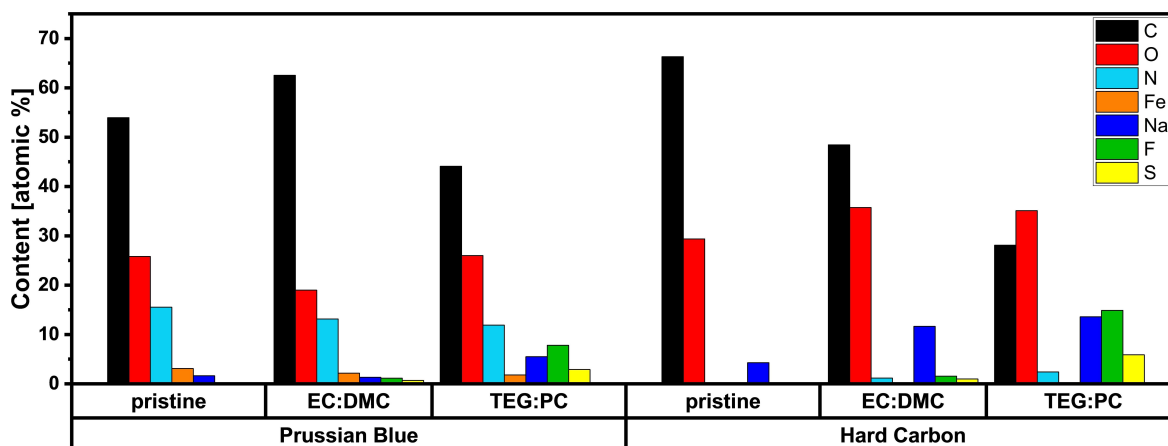


Figure 6. Composition of pristine PB and HC electrodes, as well as PB and HC electrodes after 1000 charge-discharge cycles in NIB full cells with TEG/PC and EC/DMC electrolyte, determined by XPS.

SEI layer is generally thicker in the TEG/PC electrolyte, compared to EC/DMC. This finding is in line with the results of a previous study, investigating the use of glyoxylic-acetal-based electrolytes in combination with silicon-graphite composite electrodes in LIB: Comparative XPS analysis showed that the SEI layer formed on the electrode surface is thicker if LiTFSI in TEG is used instead of LP30 or LiTFSI in EC/DMC (1:1).^[10] This thicker and smoother SEI layer contributes to an increased cycling stability of cells with TEG-based electrolyte. It is thus conceivable that analogue conclusions can be drawn for the NIB investigated in this work: The thicker SEI layer may lead to additional overpotentials that cause the slightly lower capacity of HC with TEG/PC compared to EC/DMC electrolyte (compare Figure S4 of the SI). But it may have a positive impact on the cycling stability as it acts a protection layer for further electrode corrosion. Considering the corresponding C 1s, F 1s and S 2p spectra in Figure S9 in the SI, this thicker SEI layer in TEG/PC contains species like NaF, Na₂(SO₃)₂ and CF₃/CF₂ species that are responsible for the noticeable content of F and S that are observed in Figure 6. Furthermore, an increase in carbonyl functional groups can be observed, compared to the pristine HC electrode.

On the cathode side, similar observations with respect to the content of F, S and Na on the cycled electrodes can be made. After 1000 cycles with TEG/PC, higher contents of these three elements can be found, compared to the EC/DMC sample. Simultaneously, the atomic content of carbon is reduced by 10%, N by 3.5% and Fe by 1.2%, while the content of oxygen remains unchanged. In combination with the spectra shown in Figure S9 of the SI, the formation of a surface layer, containing carboxyl- and carbonyl- groups, as well as -CF₃ species can be concluded. In the case of EC/DMC, however, an increased carbon content is found alongside only small fractions of F (1.2%) and S (0.7%). The contents of O, N, Fe and Na are reduced with respect to the pristine PB electrode. Consequently, the PB electrode cycled with EC/DMC is exposed to an evolution process that reduces the amount of active material directly exposed to the surface (lower Fe and N content), while

simultaneously leading to a higher share of C and a lower share of O. Taking this into consideration, the detachment of active material from the surface, or its (partial) dissolution in the electrolyte, leaving behind the carbon conductive additive, may be possible explanations. The dissolution of transition metals from PBAs has, to the best of our knowledge, so far been only studied in aqueous electrolytes. According to the work of Lamprecht et al.,^[25] Fe can be, most likely, dissolved as the Fe(CN)₆⁴⁻ or Fe(CN)₆³⁻ complex. This process mainly depends on the pH of the electrolyte and the type of anion. Among the tested conductive salts, the lowest dissolution activities have been observed for NaClO₄ and the highest for Na₂SO₄. Furthermore, basic conditions promote the dissolution of Fe(CN)₆^{3/4-} from the structure. The structural stability of PB and its analogues in EC/DMC and other organic electrolytes might thus be a topic that should be reviewed in a larger scope in future works. This, however, reaches beyond the implementation of glyoxylic-acetals in sodium-ion energy storage systems. In scope of this work, it can be concluded that the TEG/PC electrolyte forms a protective CEI layer on the PB material used here, which is not sufficiently accomplished using EC/DMC.

The positive impact of glyoxylic-acetals on the interphase created on carbonaceous electrodes may not be exclusively relevant for NIB or alkali-metal-ion batteries in general but can be applied for the realization of other energy storage devices relying on this type of negative electrode. Hybrid devices, i.e., alkali metal ion capacitors, combine a battery electrode, originally the negative electrode, with an activated carbon electrode, as it is used in supercapacitors.^[26] By this approach, the gap between batteries, excelling in energy density and supercapacitors, excelling in power density, may be covered. Figure 7 demonstrates that the preformed HC electrodes that were used for the assembly of NIB discussed before, can be also used as negative electrode in a sodium-ion capacitor (NIC), if they are pre-doped with sodium-ions. In this experiment, commercial activated carbon was used as the positive electrode. By adjusting the potential of the latter via pre-cycling to around 3.5 V, both electrodes are brought to a suitable

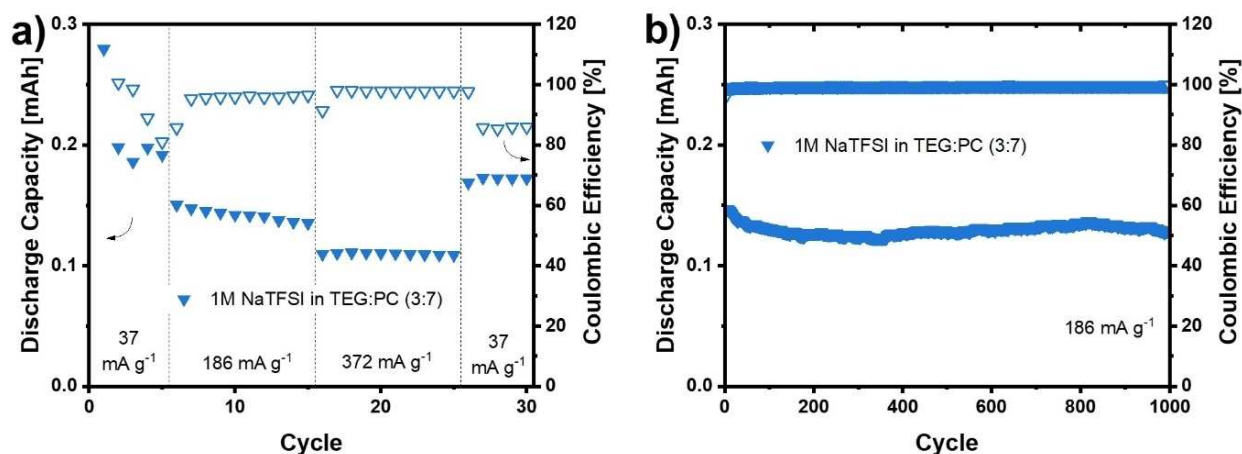


Figure 7. a) Rate capability and b) cycling stability of a sodium-ion capacitor with 1 M NaTFSI in TEG/PC (3:7) as electrolyte.

potential window, resulting in a voltage range of 0.75 to 3.55 V at 186 mA g^{-1} for the device (Figure S7 of the SI). The rate capability of this non-optimized lab-scale device (Figure 7a) is limited by the HC material in the first place. It may be improved by increasing its mass ratio, but an optimization towards high power performance would require an optimization of the negative electrode material to provide faster cation diffusion kinetics. Recently, it has been demonstrated that NICs containing N/S-co-coped carbon nanoparticles as negative electrode and activated carbon nanoparticles as positive electrode can retain 60% of the capacity, when increasing the current density from 0.1 to 10 Ag^{-1} .^[27] Here, the focus shall be placed on the characterization of electrolytes using glyoxylic acetals as solvents and electrode material development is therefore out of the scope of this work. Nevertheless, a comparison of the TEG/PC-NIC rate test (Figure 7a) with the TEG/PC-NIB rate test in Figure 5a, reveals that the capacity retention from highest to lowest rate is improved from 37% to 56% when changing the setup from battery to hybrid device. Furthermore, the resulting NIC is capable of being charged and discharged for 1000 times providing a capacity retention of 85% (Figure 7b), which once more demonstrates that the glyoxylic acetal containing electrolyte can provide a stable long-term cycling performance, including the formation of stable interphases on the electrode material (compare Figure S10 of SI for XPS spectra). Future investigations, using alternative electrode materials, are however required to further investigate the performance of glyoxylic acetal electrolytes in high power devices especially at current densities above 1 Ag^{-1} .

Conclusion

This work showed that the advantageous properties of glyoxylic-acetals as electrolyte solvents can be utilized in sodium-ion energy storage devices. Compared to electrolytes containing volatile linear carbonates, formulations based on 1,1,2,2-tetramethoxyethane (TMG), 1,1,2,2-tetraethoxyethane

(TEG) or a mixture of TEG with a cyclic carbonate (propylene carbonate, PC), exhibit increased thermal stabilities and higher flash points. By introducing PC as co-solvent, the ionic conductivity, as well as anodic electrochemical stability of sodium-glyoxylic-acetal electrolytes can be improved, enabling their use in combination with high operating voltage cathodes.

Towards implementation of this electrolyte in sodium-ion energy storage systems, the performance of TEG/PC in Prussian Blue (PB) and hard carbon (HC) half-cells was compared to EC/DMC. Despite the slightly higher capacity of HC with the conventional carbonate electrolyte, the formulation containing glyoxylic-acetal could prove as competitive in terms of capacity and rate capability, even enabling higher Coulombic efficiency of Na de-/intercalation in PB. On the full cell level, cells with TEG/PC provide around 80% of the capacity that is obtained with EC/DMC. Most noticeably, the galvanostatic cycling of sodium-ion full-cells over 1000 cycles revealed a strongly increased capacity retention if TEG/PC is used as electrolyte. The thicker and presumably more protective interphases formed with TEG/PC and possibly its lower susceptibility to degradation reactions in the cell, might explain this observation. Especially on the cathode side, this electrolyte seems to suppress aging mechanisms that occurred when combining the used PB material with the EC/DMC electrolyte.

We furthermore demonstrated that glyoxylic-acetal electrolytes can be utilized in sodium-ion capacitors, providing a high cycling stability. These results confirm that glyoxylic-acetals are promising solvents not only for lithium- and potassium-, but also for sodium-ion batteries and capacitors. Their thermal stability and film-forming ability, establishing protective electrode-electrolyte interphases, represent key advantages for the realization of safe and durable sodium-ion energy storage devices.

Acknowledgements

The authors wish to thank the Thüringer Ministerium für Wirtschaft, Wissenschaft und Digitale Gesellschaft (TMWWDG), and the Thüringer Aufbau Bank (TAB) within the project LiNaKon (2018 FGR 0092) and the DFG Research Infrastructure Grant (INST 275/257-1 FUGG) for the financial support. We further acknowledge support by the European Fonds for Regional Development (Europäischer Fonds für Regionale Entwicklung; EFRE-OP 2014-2020; Project No. 2021 FGI 0035, NanoLabXPS) as part of the REACT-EU program.

The authors would also like to thank Beate Fähndrich for her support on the TGA measurements, as well as Lukas Köps for providing and maintaining data evaluation and storage infrastructure. Open Access funding enabled and organized by Projekt DEAL.

Conflict of Interests

The authors declare no conflict of interest.

Data Availability Statement

The data that support the findings of this study are available from the corresponding author upon reasonable request.

Keywords: Energy storage · sodium-ion battery · sodium-ion capacitor · glyoxal · electrolyte

- [1] A. Eftekhari, D.-W. Kim, *J. Power Sources* **2018**, *395*, 336–348.
- [2] A. Rudola, A. J. R. Rennie, R. Heap, S. S. Meysami, A. Lowbridge, F. Mazzali, R. Sayers, C. J. Wright, J. Barker, *J. Mater. Chem. A* **2021**, *9*, 8279–8302.
- [3] a) C. Vaalma, D. Buchholz, M. Weil, S. Passerini, *Nat. Rev. Mater.* **2018**, *3*, 18013; b) P. K. Nayak, L. Yang, W. Brehm, P. Adelhelm, *Angew. Chem. Int. Ed.* **2017**, *57*, 102.
- [4] a) Altris AB “Fennac.” can be found under <http://www.altris.se/fennac/> (accessed 11.08.22); b) HiNa Battery Technology Co., Ltd “R&D achievements.” can be found under <http://www.hinabattery.com/en/index.php?catid=15> (accessed 11.08.22); c) Faradion Limited “Reliance New Energy Solar to Acquire Faradion Limited.” can be found under <https://faradion.co.uk/reliance-new-energy-solar-to-acquire-faradion-limited/> (accessed 11.08.22); d) AMTE Power “AMTE Power announces a collaboration and licensing deal with Faradion, a world leader in sodium-ion battery technology.” can be found under <https://amte-power.com/amte-power-announces-a-collaboration-and-licensing-deal-with-faradion-a-world-leader-in-sodium-ion-battery-technology/> (accessed 11.08.22); e) CATL “CATL Unveils Its Latest Breakthrough Technology by Releasing Its First Generation of Sodium-ion Batteries.” can be found under <http://www.catl.com/en/news/665.html> (accessed 11.08.22).
- [5] G. G. Eshetu, G. A. Elia, M. Armand, M. Forsyth, S. Komaba, T. Rojo, S. Passerini, *Adv. Energy Mater.* **2020**, *10*, 2000093.
- [6] a) G. Heydrich, I. Richter, T. Krug, BASF Aktiengesellschaft, Germany, **2005**; b) J. Ruwwe, J. Bruehl, C. Osterholt (Degussa A.-G., Germany), EP-A1 1460052, **2004**.
- [7] L. H. Heß, A. Balducci, *ChemSusChem* **2018**, *11*, 1919–1926.
- [8] J. M. Bernard, A. Jomier (Rhodia Operations, France), US-B2 8981032, **2008**.
- [9] a) L. H. Hess, S. Wankmüller, L. Köps, A. Bothe, A. Balducci, *Batteries & Supercaps* **2019**, *2*, 852–857; b) C. Leibing, A. Balducci, *J. Electrochem. Soc.* **2021**, *168*, 090533; c) L. Medenbach, L. C. Meyer, A. Balducci, *Electrochem. Commun.* **2021**, *125*, 107001.
- [10] L. Gehrlein, C. Leibing, K. Pfeifer, F. Jeschull, A. Balducci, J. Maibach, *Electrochim. Acta* **2022**, *424*, 140642.
- [11] A. Bothe, L. Gehrlein, Q. Fu, C. Li, J. Maibach, S. Dsoke, A. Balducci, *Batteries & Supercaps* **2022**, *5*, e202200152.
- [12] a) J. Atik, S. Röser, R. Wagner, D. Berghus, M. Winter, I. Cekic-Laskovic, *J. Electrochem. Soc.* **2020**, *167*, 040509; b) L. Köps, C. Leibing, L. H. Hess, A. Balducci, *J. Electrochem. Soc.* **2021**, *168*, 010513; c) S. Liu, L. C. Meyer, L. Medenbach, A. Balducci, *Energy Storage Mater.* **2022**, *47*, 534–541.
- [13] S. D. Magar, C. Leibing, J. L. Gómez-Urbano, D. Carriazo, A. Balducci, *Energy Technol.* **2022**, *10*, 2200379.
- [14] G. G. Eshetu, S. Grugeon, H. Kim, S. Jeong, L. Wu, G. Gachot, S. Laruelle, M. Armand, S. Passerini, *ChemSusChem* **2016**, *9*, 462–471.
- [15] D. Monti, E. Jónsson, A. Boschini, M. R. Palacin, A. Ponrouch, P. Johansson, *Phys. Chem. Chem. Phys.* **2020**, *22*, 22768–22777.
- [16] K. Xu, *Chem. Rev.* **2014**, *114*, 11503–11618.
- [17] Y. Lyu, Y. Liu, Z.-E. Yu, N. Su, Y. Liu, W. Li, Q. Li, B. Guo, B. Liu, *Sustain. Mater. Technol.* **2019**, *21*, e00098.
- [18] J. Xiao, X. Li, K. Tang, D. Wang, M. Long, H. Gao, W. Chen, C. Liu, H. Liu, G. Wang, *Mater. Chem. Front.* **2021**, *5*, 3735–3764.
- [19] a) A. Bauer, J. Song, S. Vail, W. Pan, J. Barker, Y. Lu, *Adv. Energy Mater.* **2018**, *8*, 1702869; b) W. Wu, S. Shabagh, J. Chang, A. Rutt, J. F. Whitacre, *J. Electrochem. Soc.* **2015**, *162*, A803–A808.
- [20] J. Peng, W. Zhang, Q. Liu, J. Wang, S. Chou, H. Liu, S. Dou, *Adv. Mater.* **2022**, *34*, 2108384.
- [21] Y. Jiang, S. Yu, B. Wang, Y. Li, W. Sun, Y. Lu, M. Yan, B. Song, S. Dou, *Adv. Funct. Mater.* **2016**, *26*, 5315–5321.
- [22] Y. You, H.-R. Yao, S. Xin, Y.-X. Yin, T.-T. Zuo, C.-P. Yang, Y.-G. Guo, Y. Cui, L.-J. Wan, J. B. Goodenough, *Adv. Mater.* **2016**, *28*, 7243–7248.
- [23] I. Hasa, S. Mariyappan, D. Saurel, P. Adelhelm, A. Y. Kozlov, C. Masquelier, L. Croguennec, M. Casas-Cabanias, *J. Power Sources* **2021**, *482*, 228872.
- [24] M. Zhang, Y. Li, F. Wu, Y. Bai, C. Wu, *Nano Energy* **2021**, *82*, 105738.
- [25] X. Lamprecht, F. Speck, P. Marzak, S. Cherevko, A. S. Bandarenka, *ACS Appl. Mater. Interfaces* **2022**, *14*, 3515–3525.
- [26] a) G. G. Amatucci, F. Badway, A. Du Pasquier, T. Zheng, *J. Electrochem. Soc.* **2001**, *148*, A930; b) K. Kuratani, M. Yao, H. Senoh, N. Takeichi, T. Sakai, T. Kiyobayashi, *Electrochim. Acta* **2012**, *76*, 320–325; c) S. Komaba, T. Hasegawa, M. Dahbi, K. Kubota, *Electrochem. Commun.* **2015**, *60*, 172–175.
- [27] N. Diez, M. Sevilla, A. B. Fuertes, *Carbon* **2023**, *201*, 1126–1136.

Manuscript received: February 3, 2023
 Revised manuscript received: March 10, 2023
 Accepted manuscript online: March 22, 2023
 Version of record online: March 22, 2023